Hindawi Publishing Corporation
Journal of Nanotechnology
Volume 2012, Article ID 237284, 12 pages
doi:10.1155/2012/237284

Research Article

Responses of Algal Cells to Engineered Nanoparticles Measured as Algal Cell Population, Chlorophyll a, and Lipid Peroxidation: Effect of Particle Size and Type

D. M. Metzler,[1] A. Erdem,[2] Y. H. Tseng,[3] and C. P. Huang[1]

[1] *Department of Civil and Environmental Engineering, University of Delware, Newark, DE 19716, USA*
[2] *Department of Environmental Engineering, Akdeniz University, Akdeniz 07058, Turkey*
[3] *Department of Chemical Engineering, National Taiwan University of Science and Technology, Taipei 106, Taiwan*

Correspondence should be addressed to C. P. Huang, huang@udel.edu

Received 15 May 2012; Accepted 24 July 2012

Academic Editor: Mallikarjuna Nadagouda

Copyright © 2012 D. M. Metzler et al. This is an open access article distributed under the Creative Commons Attribution License, which permits unrestricted use, distribution, and reproduction in any medium, provided the original work is properly cited.

This paper investigated toxicity of three engineered nanoparticles (ENP), namely, Al_2O_3, SiO_2, and TiO_2 to the unicellular green algae, exemplified by *Pseudokirchneriella subcapitata* with an emphasis on particle size. The changes in pH, cell counts, chlorophyll a, and lipid peroxidation were used to measure the responses of the algal species to ENP. The most toxic particle size was TiO_2 at 42 nm with an EC20 of 5.2 mg/L and Al_2O_3 at 14–18 nm with an EC20 of 5.1 mg/L. SiO_2 was the least toxic with an EC20 of 318 mg/L. Toxicity was positively related to the surface charge of both ENP and algae. The chlorophyll content of the algal cells was influenced by the presence of ENP, which resulted in limited light and availability of nutrients due to increase in turbidity and nutrient adsorption onto the ENP surface, separately. Lipid peroxidation was attributed to reactive oxygen species (ROS). Fast reaction between algal cells and ROS due to direct contact between TiO_2 and algal cells is an important factor for lipid peroxidation.

1. Introduction

Nanomaterials have been used in industrial applications and commercial products at a rapid pace. New types of NM are being developed every day. These new materials can be more hazardous than their bulk states due to not only small size but also numeral novel properties. Among these particles, TiO_2, SiO_2, and Al_2O_3 have been shown to have adverse effects on the pulmonary systems [1–3]. There have been a few studies on the effect of these particles on algae. Van Hoecke et al. [4] observed changes in the growth rate of *P. subcapitata* when exposed to SiO_2. Warheit et al. [5] reported growth inhibition of *P. subcapitata* with a 72-hour EC50 of 87 and 61 mg/L for TiO_2 at size of 38.5 and 100 nm, respectively. Ji et al. [6] reported a 6-day survival EC50 of 120 mg/L for anatase with a size of 20–50 nm. Literature results so far have indicated a clear dose-response relationship between microbial survival and ENP concentration. However, more studies are needed to illustrate the mechanisms of microbial responses to ENP.

Reactive oxygen species (ROS) are generated in the thylakoid membrane during photosynthesis [7]. Hydrogen peroxide has been suggested to be the dominant species of ROS in algae. This is due to relatively long reaction time involving hydrogen peroxides, approximately 1 millisecond compared to nanoseconds of other ROS species. The ROS-protective mechanisms of algae include superoxide dismutase, ascorbate peroxidase, catalase, and glutathione peroxidase [7]. The photoactivity of TiO_2 also generates ROS. The generation of ROS has also been linked to particle size, crystalline structure, and surface defects [8]. The particle size is an important variable in that as the specific surface area increases reversely proportionally to particle diameter. The increase in specific surface area will result in the increase in specific quantum yield of photocatalytic particles thus increasing the ROS generation [9–11]. Bakardjieva et al. [10] demonstrated that as the specific surface area of TiO_2 increased, 4-chlorophenol degradation increased. Tesng et al. [9] indicated that 2-chlorophenol degradation decreased with increased primary particle size. The size effect on photoctalytic capacity has been

seen in other particles including CdS [12], HgSe and PbSe [13], ZnO [14], and SnO_2 [15]. It was concluded that particle size of quantum dots is one major factor affecting cytotoxicity [16]. Kashiwada [17] demonstrated that latex nanoparticle was adsorbed to spawned ST II eggs at an optimum particle size of 474 nm. Adams et al. [18] examined the effect of particle size of TiO_2, SnO_2, and ZnO on *B. subtilis* and *E. coli* and observed some degree of toxicity whether the particles were under light or not. However, they were unable to draw conclusion about the particle size effect due to the change of particle size once in suspension.

The objective of this study was to determine the toxicity of photocatalytic (e.g., TiO_2) and non-photocatalytic nanoparticles (e.g., Al_2O_3 and SiO_2) over a wide range of particle size by evaluating the effects on cell population, chlorophyll, and lipid peroxidation on *P. subcapitata*. The mode of toxicity was also examined.

2. Methods and Materials

2.1. Nanoparticles. Stock suspensions of 2 g/L were made with aluminum oxide, silica dioxide, or titanium dioxide in 150–500 mL of Erlenmeyer flask with algal growth medium [19]. Table 1 gives the information about the physical and chemical properties of ENP materials studied. The stock suspensions were autoclaved for 20 minutes at 120°C at least one day prior to experiment and stored at room temperature until use.

2.2. Algal Culture. Algal culture, *P. subcapitata,* was purchased from Aquatic Biosystems (Fort Collins, CO). The algal inoculums were stored at 4°C in the dark for no longer than 6 months. Culturing of the algae in 3 L continually stirred tank reactor (CSTR) followed that of Metzler [20]. Hydraulic residence time (HRT) of the CSTR was 3 days, with a flow rate of 50 mL/h.

2.3. Growth Chambers. Growth chambers were approximately 80 cm × 62 cm × 68 cm, wood or metal frame that was covered in black cloth. A bank of 6 fluorescent lights was suspended overhead on the frame. Lights used included model GE PL/AQ F12T20 (General Electric, Fairfield, CT), Gro-lux F12T20/Gro/AQ, and 2 Sylvania Gro-lux wide spectrum F12T20/Gro/AQ/WS (Rutherford, NJ, USA). These light fixtures supplied an average lux of 1632 ± 157, measured from the top of the test beakers. A muffin fan or centrifugal miniblower removed excess heat generated by the lights. Each fan or blower used was suspended on the outside of the chamber approximately 1 inch below the lights, with an access port cut into the cloth. An orbital platform shaker held the beakers and was set to oscillate at 150 rpm.

2.4. Exposure Experiments. Aliquots of stock NP were added to a series of 1 L beakers. Stock suspensions were continuously stirred with a magnetic stirring bar during this time. Algal growth medium was then added to the beakers to bring the volume to 100 mL. The suspensions were sonicated for 2 minutes at a power level of 48 W using a Cole-Palmer 4710 series ultrasonic homogenizer. The suspensions were then allowed to equilibrate for one hour. After one hour, 100 mL of the CSTR algal culture was added to the NP suspension to achieve an algal cell density of $1.4 \pm 0.9 \times 10^6$ cell/mL. The samples were then placed in one of three growth chambers. The duration of the exposure test was 4 days.

Each day during the course of exposure experiment the sample pH was measured with a Corning pH/ion analyzer 350 equipped with a Corning semimicro combo pH probe. Additionally, the minimum and the maximum temperatures of the growth chambers were recorded for each 24-hour time period. At the end of the 4-day exposure, the sample volume remaining was determined by measuring the difference in volume before and after exposure runs. Forty milliliters of sample were collected in 50 mL Fisherbrand centrifuge tubes which were analyzed for chlorophyll a. Additionally, 12 mL were collected in 15 mL Fisherbrand centrifuge tubes and analyzed for cell density and lipid peroxidation. The samples were stored at 4°C in the dark (a maximum of 7 days) until analyzed. According to Weber et al. [21], no changes in chlorophyll content should occur of this time period.

Cell densities were measured by direct cell counts. One milliliter of sample was diluted in 1 mL of 0.5 M lauryl sulfate. This was then mixed on a Dade vortex shaker model S8223-1 for 2 minutes. An aliquot of sample was then added to a hemocytometer for counting on an Olympus AX70 microscope; samples were counted a minimum of 4 times. Cell densities were converted into total cell population by multiplying the cell counts by the volume of sample remaining in the 1 L test beakers at the end of the test duration. The total cell populations were then corrected for the initial population and normalized based on the control, using the following equation:

$$R_s = \frac{(\rho \times v)_t}{(\rho \times v)_c}, \tag{1}$$

where R_s is the normalized growth, ρ is the cell density (cell/mL), v is the volume of sample at the end of the 4-day exposure period (mL), t is the duration a sample was exposed to a specific ENP, and c is the control sample with no treatment.

For the determination of chlorophyll a, the samples were concentrated to between 0.5–3 mL, and then analyzed according to Standard Methods for the Examination of water and Wastewater [22]. In brief, the concentrated samples were added to glass homogenization tubes. The 50 mL sample tubes were rinsed with a few milliliters of Mg acetone (2.0 g of $(MgCO_3)_4$ and $Mg(OH)_2 \cdot 5H_2O$ diluted to 200 mL in distilled deionized water then diluted 1 : 10 in acetone). The volume in the homogenization tube was brought to 3 mL with Mg-acetone solution. The samples were then homogenized for 1 minute at 2000 rpm with a Glas-Col variable speed-reversible homogenizer. The samples were then steeped at 4°C in the dark for 2 hours in 15 mL plastic centrifuge tubes. After the steep time, the samples were centrifuged for 30 minutes at 664 ×g. The optical density of the supernatant was measured at 750 and 664 nm, respectively, on a Hewlett-Packard UV-Vis model 8525A. HCl (0.1 mL of 0.1 N) were added to the samples and the optical density was measured

Table 1: Nanoparticles used in the present study.

Type	Name	Source	Method of production	ID	Density (g/cc)[a]	Surface area (m^2/g)	Surface charge (pH_{pzc})[b]	Diameter (nm)[c]
Silica dioxide (SiO_2)	Aerosil 90	Degussa Corp.	Continuous flame hydrolysis	Aero90	2.2	76.5	2.0	35.6
	Aerosil 130	Degussa Corp.		Aero130	2.2	105.1		26
	Aerosil 200	Degussa Corp.		Aero200	2.2	190.6		14.3
	Aerosil 300	Degussa Corp.		Aero300	2.2	284.8		9.6
Aluminum oxide (Al_2O_3)	Standard alumina powder	Allied High Tech Products	Proprietary calcining	Std Al	3.69	24.1	8.2–9.1	67.5
	Alumina			Al1520	3.69	92.3		17.6
	Gamma alumina powder, type N	Allied High Tech Products	Proprietary calcining	Al γ-α	3.69	102.9		15.8
Titanium dioxide (TiO_2)	8–840	University of Delaware	Temperature annealing	8-840	3.9	7.5	5.4–6.5	204.1
	9–780			9-780	3.9	12.6 ± 0.9c		122.3
	7–660			7-660	3.9	33.6		45.8
	SL1		Sol-gel	SL1	3.9	36.2		42.5
	10–600		Temperature annealing	10-600	3.9	36.6		42
	P25	Degussa Corp.	Liquid-gas phase synthesis	P25	3.9	44.0 ± 2.9c		35.1
	SL2	University of Delaware	Sol-gel	SL2	3.9	87.7		30.3
	Wo5	Dong et al. [63]	Reverse micelle	Wo5	3.9			18.7
	Reade 5	Nanostructured and Amorphous Materials, Inc.	Wet-chemistry precipitation	R5	3.9	290.5 ± 8.2c		5.3
	Reade 10	Nanostructured and Amorphous Materials, Inc.	Wet-chemistry precipitation	R10	3.9	319.3		4.8
	U100	Sachtleben Chemicals	Sol-gel	U1100	3.9	322.4		4.8

a: references for NP density: (TiO_2) [31], [63]; (SiO_2) [64] (Al_2O_3) [64, 65].
b: references for surface charges (Al_2O_3 and SiO_2) [30]; (TiO_2) [66].
c: diameter of NP calculated from $r = 3/(\rho \times \Sigma \times 10^6)$; where r is the diameter of the particle (nm), ρ is the density of the particle (g/cm^3), and Σ is the specific surface area of the NP (m^2/g) measured by N_2-BET.
d: 9–780, P25, and R5 were measured in triplicate ±1 standard deviation shown.

again at 750 and 665 nm after 90 seconds of equilibration. The concentration of chlorophyll a ([Chla] in mg-Chla/m^3) was calculated by the following equation:

$$[\text{Chla}] = 26.7(A_{664} - A_{665}) \times V_1 \times (V_2 \times l)^{-1}, \quad (2)$$

where A_{665} is the absorbance at 664 nm before adding acid, A_{665} is the absorbance at 665 nm after adding acid, V_1 is the volume of extract (L), V_2 is the sample volume (m^3), and l optical path (cm). The specific chlorophyll a was calculated by the following expression:

$$y = [\text{Chla}] \times \rho^{-1} \times 10^{-6}, \quad (3)$$

where y is the specific chlorophyll a (mg Chla/cell), [Chla] is the concentration of chlorophyll a (mg Chla/m^3), and ρ is the cell density (no. cell/mL). The specific chlorophyll a, y, was then normalized with respect to the control according to the following equation:

$$Y = y \times {y_c}^{-1}, \quad (4)$$

where Y is the normalized specific chlorophyll a (dimensionless), y is the specific chlorophyll a (mg Chla/cell), and y_c is the specific chlorophyll a of the control (mg Chla/cell).

Finally, analysis of sample for lipid peroxidation followed the method in Maness et al. [23]. In brief, 1 mL of sample was added to 2 mL of 10% trichloroacetic acid. The samples were then centrifuged for 45 minutes at 11000 ×g. The supernatant was then added to 3 mL of 6.7 g/L 2-thiobarbituric acid, which was previously heated to 60°C in order to dissolve the solid. The samples were then heated in boiling water for 10 minutes. After cooling, the absorbance of samples was measured on a Hewlett-Packard UV-Vis model 8525A at 532 and 600 nm wavelengths, respectively. The absorbance at 532 nm was corrected for the background at 600 nm. Calibration standards were made from 1,1,3,3-tetramethoxypropane. The specific lipid peroxidation (z) was calculated by the following equation:

$$z = [\text{MDA}] \times \nu \times (\rho \times \nu)^{-1} \times 10^{-3}, \quad (5)$$

where z has the unit of pmol MDA/cell, [MDA] is the concentration of malondialdehyde-thiobarbituric acid complex measured (μM), ν is the volume of sample at the end of the 4 day exposure (mL), and ρ is the cell density (no. cell/mL). The z value was then normalized against the control according to the following equation:

$$Z = z \times {z_c}^{-1}, \quad (6)$$

where Z is relative lipid peroxidation (dimensionless), z is the specific lipid peroxidation of the sample (pmol MDA/cell), and z_c is the specific lipid peroxidation of the control (pmol MDA/cell).

Dose-response curves were used to calculate the effective concentration (EC). The USEPA [19] uses daily cell density to calculate the growth inhibition concentration (IC). The number of samples to be processed per day made this impractical. Lethal concentration (LC) values, defined as the total number of organisms that died during exposure, were not used to determine the toxicity of NP to algae. Therefore, EC was chosen. EC value is defined as the difference in total growth between control and test sample. EC20 and EC50 are concentrations that limit growth to 20 and 50% of the control samples.

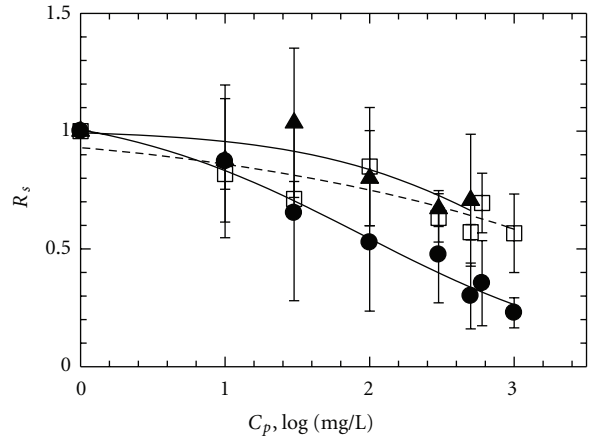


Figure 1: Normalized specific four-day growth (R_s) dose-response curve. Solid circles are Al_2O_3 (17.6 nm). Open squares are SiO_2 (14.3 nm). Solid triangles are TiO_2 (18.7 nm). Error bars are ±1 standard deviation ($n \geq 3$). Lines represent four-parameter logistic curves fitted to the data in SigmaPlot ver. 9.01. Experimental conditions: initial algae concentration = $1.4 \pm 0.9 \times 10^6$ cell/mL, test duration = 4 days, and initial test volume = 200 mL.

3. Results

The size and type are important attributes of ENP. The major objective of the present research was to determine how particle size and type will affect the physiology and biochemical behavior of algae exemplified by *P. subcapitata*. The algal cells were exposed to TiO_2, Al_2O_3, and SiO_2 for 96 h at various size classes and concentrations. During the time of exposure, the average temperature was 23.0 ± 1.2°C and the average pH was 7.6 ± 0.4.

3.1. Effect of Particle Concentration. In order to determine the effect of NP concentration on *P. subcapitata*, Al_2O_3 (17.6 nm), SiO_2 (14.3 nm), and TiO_2 (18.7 nm) were selected due to their similarity in size. Figure 1 shows the dose-response curves of Al_2O_3, SiO_2, and TiO_2 in terms of normalized specific growth (R_s). In all cases, as concentration increased from 0 to 1000 mg/L, the R_s decreased. EC20 values were calculated using SigmaPlot version 9.01 as follows: Al_2O_3 (17.6 nm) = 5.14 mg/L, TiO_2 (18.7 nm) = 129 mg/L, and SiO_2 (14.3 nm) = 318 mg/L.

Chlorophyll content of algae can be used as a measurement of physiological health [22]. In order to determine if NP was stressing the algae, chlorophyll a measurements were conducted. Figure 2 shows chlorophyll a content plotted against the concentrations of the respective NP. It can be seen that there was a slight increase in the chlorophyll content as the Al_2O_3 concentration was increased to about 10 mg/L.

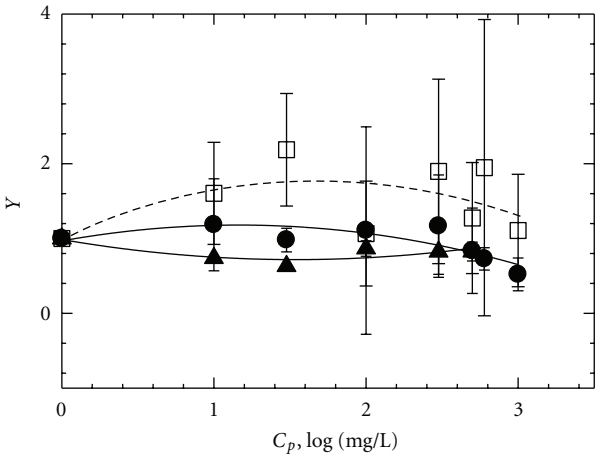


Figure 2: Normalized specific chlorophyll a (Y) as a function of the concentration of the NP. Solid circles are Al_2O_3 (17.6 nm). Open squares are SiO_2 (14.3 nm). Solid triangles are TiO_2 (18.7 nm). Error bars are ±1 standard deviation ($n \geq 3$). Lines are 2nd-order polynomial fits to the data. The data was fitted with an empirical 2nd-order polynomial from SigmaPlot ver. 9.01. Experimental conditions: initial algae concentration = $1.4 \pm 0.9 \times 10^6$ cell/mL, test duration = 4 days, and initial test volume = 200 mL.

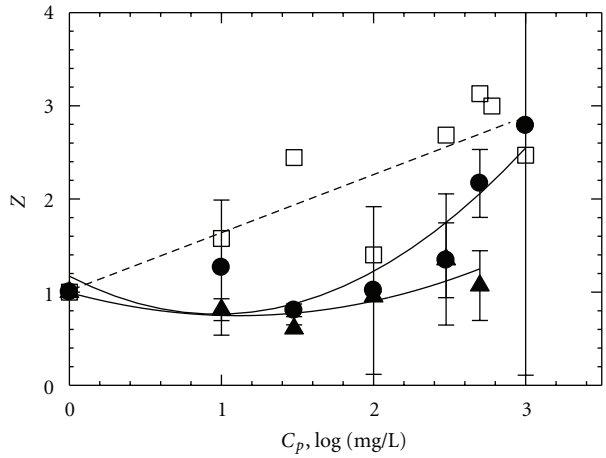


Figure 3: Normalized specific lipid oxidation (Z) as a function of the concentration NP. Solid circles are Al_2O_3 (17.6 nm). Open squares are SiO_2 (14.3 nm). Solid triangles are TiO_2 (18.7 nm). Error bars are ±1 standard deviation. Error bars were omitted from SiO_2 plot. Lines are 2nd-order polynomial fits to the data. Experimental conditions: initial algae concentration = $1.4 \pm 0.9 \times 10^6$ cell/mL, test duration = 4 days, and initial test volume = 200 mL.

As the Al_2O_3 (solid circles) concentration was increased above 10 mg/L, the chlorophyll content decreased to approximately 50% of the control at 1000 mg/L of Al_2O_3. As SiO_2 (open squares) concentration was increased from 0 to 30 mg/L, the Chla increased from 1 to 2.2. The Chla then decreased to 1 at 1000 mg/L of SiO_2. The NP of TiO_2 (solid triangles) had the inverse effect of Al_2O_3 and SiO_2. The Chla decreased from 1 to 0.63 when TiO_2 concentration was increased from 0 to 30 mg/L. At TiO_2 concentration greater than 30 mg/L the Chla increased to 0.83 at 1000 mg/L.

Figure 3 shows the normalized specific MDA, Z, as a function of ENP concentration for SiO_2 (open squares), Al_2O_3 (solid circles), and TiO_2 (solid triangles). The normalized specific MDA increased with the log concentration of SiO_2. The maximum normalized specific MDA, 3.1 ± 1.3, occurred at 500 mg/L of SiO_2. However, the SiO_2 results are not significantly different ($\alpha = 0.05$) from those of TiO_2 and Al_2O_3 due to large standard deviations in the data. Error bars were not shown in Figure 3 for SiO_2 due to large values. Al_2O_3 caused an increased normalized specific MDA only at concentration >100 mg/L. The maximum normalized specific MDA was 2.8 ± 2.7 at 1000 mg/L of Al_2O_3. For TiO_2 (Figure 3) normalized specific MDA decreased from 1 to 0.61 when the TiO_2 concentration was increased from 0 to 30 mg/L, respectively. At concentrations greater than 30 mg/L, the normalized specific lipid peroxidation increased until a maximum of 1.8 ± 1.4 at 600 mg/L was reached for TiO_2. The increase in normalized specific MDA was most likely due to photocatalytic properties of the TiO_2.

3.2. Particle Size Effect. In order to determine how particle size affects the toxicity of titanium dioxide, algae was exposed to TiO_2 at particle size in the range between 5.3 and 204 nm.

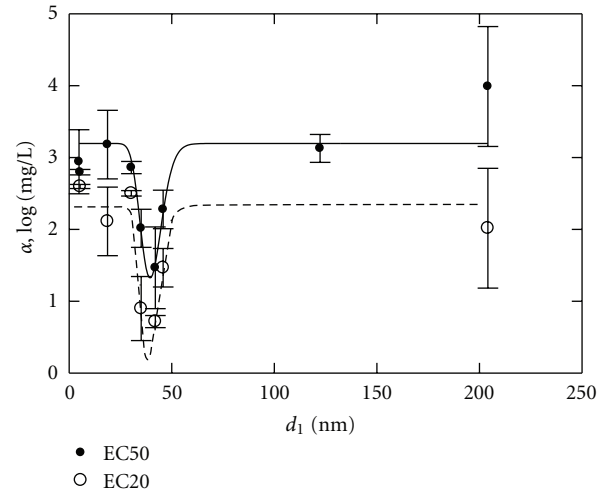


Figure 4: Critical specific growth (α) as a function of primary particle size of TiO_2 in terms of EC20 and EC50. Lines are a five-parameter modified log normal empirical fitting (7) from SigmaPlot ver. 9.01 for EC20 (dotted) and EC50 (solid). Error bars are ±1 standard deviation. Experimental conditions: initial algae concentration = $1.4 \pm 0.9 \times 10^6$ cell/mL, test duration = 4 days, and initial test volume = 200 mL.

EC20 and EC50 were calculated with Toxicity Relationship Analysis Program ver. 1 (TRAP) [24] using the logistic equation. Figure 4 gives the EC20 and EC50 values as a function of the primary NP size (d_1) exemplified by TiO_2. As the ENP size increased from 5.3 to 41 nm both, EC20 and EC50 decreased. A minimum EC20 of 5.2 mg/L and a minimum EC50 of 25.5 mg/L were observed at 42 nm primary particle size. The EC50 and EC20 then increased at $d_1 > 42$ nm. Warheit et al. reported 72-h growth EC50

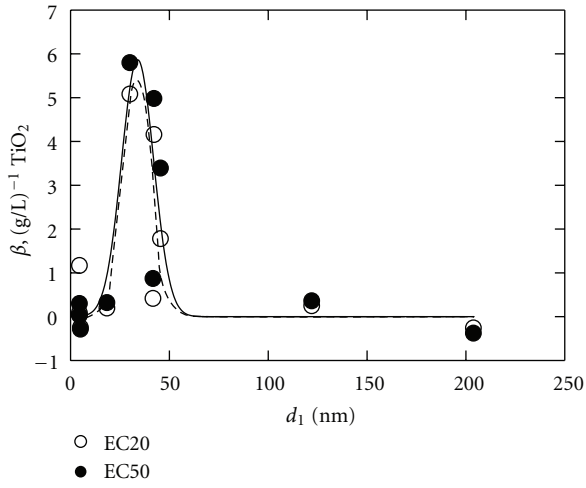


Figure 5: Critical specific chlorophyll a content (β) as a function of primary particle size of TiO_2 in terms of EC20 and EC50. Lines are fitted 3-parameter Gaussian equation (7) in SigmaPlot ver. 9.01 for EC20 (dotted) and EC50 (solid). Experimental conditions: initial algae concentration = $1.4 \pm 0.9 \times 10^6$ cell/mL, test duration = 4 days, and initial test volume = 200 mL.

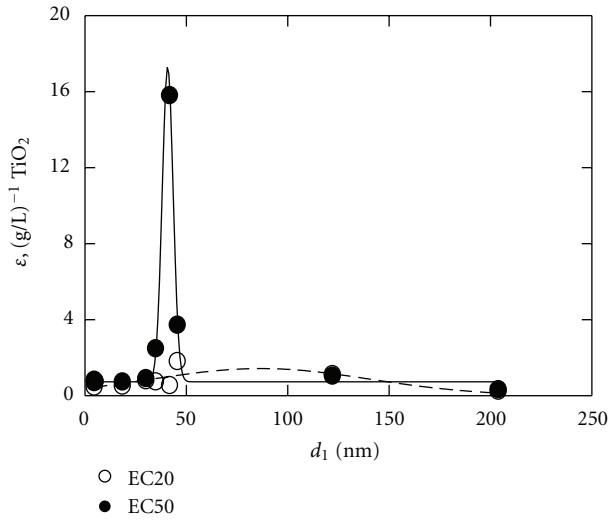


Figure 6: Critical specific lipid peroxidation (ε) as a function of primary particle size in terms of EC20 and EC50. Line is fitted 3-parameter Gaussian equation (8) in SigmaPlot ver. 9.01 for EC20 (dotted) and EC50 (solid). Experimental conditions: initial algae concentration = $1.4 \pm 0.9 \times 10^6$ cell/mL, test duration = 4 days, and initial test volume = 200 mL.

of 87 and 61 mg/L for d_1 of 38.5 and 100 nm, respectively [5]. Gonclaves et al. reported EC50 values varied between 241 mg/L and 71.1 mg/L for TiO_2 sized between 10 and 300 nm [25]. As the primary particle size increased to 204 nm the EC50 and EC20 increased to 9761.3 and 103.7 mg/L, respectively. The results were fitted with an empirical four-parameter log-normal equation:

$$\alpha = d_1^1 + a' \exp\left\{-0.5\left[\frac{\ln(d_1/d_1^2)}{b'}\right]^2\right\}, \quad (7)$$

where α is the effect concentration at either 20 or 50%, a' is a fitted constant, b is the concentration of the most toxic ENP size, d_1 (nm) is the initial diameter of the NP, d_1^1 is the smallest d_1 (nm), and d_1^2 is the d_1 in which the minimum EC50 or EC20 occurs. The r^2 values of these regressions were 0.80 and 0.90 for EC50 and EC20, respectively. Within the range of 30 to 60 nm, EC values decreased. The average minimum EC value occurred at 39.3 ± 0.2 nm for TiO_2. The calculated minimum EC values were 1.5 mg/L for EC20 and 21 mg/L for EC50.

Figure 5 shows the effect of d_1 of nano-TiO_2 on the chlorophyll a content of the algal cells. The ordinate (β) is the slope of the Chla at the EC20 and EC50 for TiO_2 or the *critical specific chlorophyll* (CSC) at EC20 or EC50, that is, β_{20} and β_{50}, respectively. A positive β_{20} indicates increase in chla production per mass of TiO_2 at EC20 compared to the control sample; a negative value implies the opposite. As the particle size increased from 4.8 to 30.3 nm, the β_{20} and β_{50} increased from about 0 to 5.5 L/g TiO_2. The β_x reached a maximum value at 30.3 nm, then abruptly decreased as the primary particle size increased. At NP size between 4.8 and 18.7 nm, there was little difference between the control and exposure. Results clearly showed that over the primary particle size range studied, for example, 19 ~ 50 nm, the Chla production increased at EC20 and EC50. When the primary particle size was greater than ca. 150 nm, the β_{20} and β_{50} became negative, indicating a decrease in Chla. The data was empirically fitted to a three-parameter Gaussian equation (8) using SigmaPlot version 9.01, that is,

$$\beta = a'' \exp\left\{-0.5\left[\frac{\left(d_1 - d_1^3\right)}{b''}\right]^2\right\}. \quad (8)$$

The variables in (8) are as follows: a and b are fitting parameters, d_1 is the ENP size (nm), and d_1^3 is the NP size (nm) with the largest β. Fitting the data to (8) resulted in a chlorophyll production maximum at 33 nm of TiO_2. The maximum β values were 5.4 and 5.9 times the control for β_{20} and β_{50}, respectively. The model fitted the data well with an r^2 value of 0.69 and 0.73 for EC20 and EC50 data, respectively.

Figure 6 shows the effect of d_1 on the lipid peroxidation. The slope of the Z plotted against TiO_2 concentration at the EC20 and EC50 of TiO_2 was obtained. This value is the *critical specific* lipid peroxidation (ε_x) where x is the EC20 or EC50. Here ε_{20} and ε_{50} were plotted as a function of d_1. As he ENP size increased from 4.8 to 30 nm, there was little change in the ε_{20} with values between 0.54 ± 0.14 L/g TiO_2. The ε_{20} then increased to 1.78 L/g TiO_2 at d_1 of 45.8 nm. The ε_{20} then decreased to 0.22 L/g TiO_2 at d_1 of 204.1 nm. The ε_{50} data showed a significant increase in the primary particle size range between 30 and 50 nm. The maximum ε_{50}, 15.8, occurred at 42 nm. At primary particle size <30 and >50 nm, the average ε_{50} value was 0.70 ± 0.23. Both data sets in Figure 6 were fitted to (8). The fitted equation had r^2 value of 0.48 and 0.99, for ε_{20} and ε_{50}, respectively. Results showed that regardless of particle size, lipid peroxidation was increased approximately by 70% at EC50. However, there was

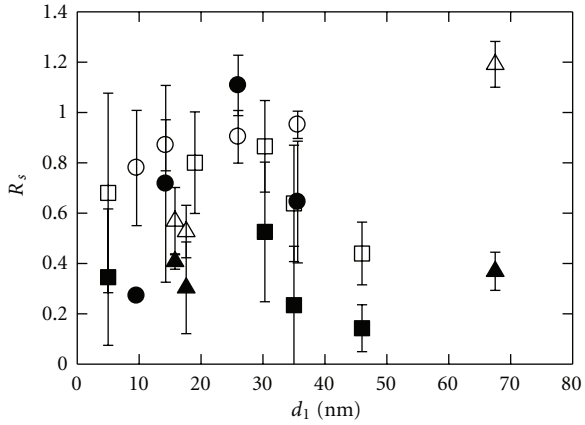


Figure 7: Normalized specific growth (R_s) for three particle-types. Circles are SiO_2, triangles are Al_2O_3, and squares are TiO_2. Open symbols are 100 mg/L of exposure dosage. Solid symbols are 1000 mg/L of exposure dosage. Experimental conditions: initial algae concentration = $1.4 \pm 0.9 \times 10^6$ cell/mL, test duration = 4 days, and initial test volume = 200 mL.

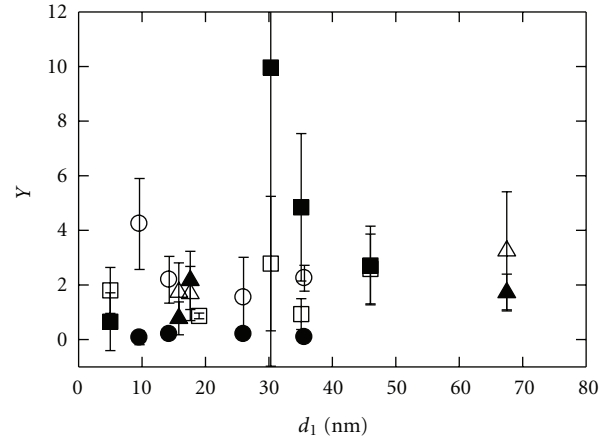


Figure 8: Normalized specific chlorophyll (Y) for three-NP samples. Circles are SiO_2, triangles are Al_2O_3, and squares are TiO_2. Solid symbols are 100 mg/L of exposure dosage. Closed symbols are 1000 mg/L of exposure dosage. Experimental conditions: initial algae concentration = $1.4 \pm 0.9 \times 10^6$ cell/mL, test duration = 4 days, and initial test volume = 200 mL.

an increase in ε_{50} between 30 and 50 nm, with a maximum of 16.6 L/g TiO_2 at 40.8 nm.

Figure 7 shows the normalized specific cell growth (R_s) in the presence of nanosized Al_2O_3, SiO_2, and TiO_2 at various d_1 values and two particle concentrations of 100 and 1000 mg/L. As the primary particle size increased from 15.8 to 67.5 nm for 100 mg/L of Al_2O_3, the NSG increased from 0.57 ± 0.13 to 1.20 ± 0.09, respectively. As SiO_2 size increased from 9.6 to 35.6 nm at 100 mg/L, the R_s increased from 0.78 ± 0.23 to 0.95 ± 0.05, respectively. R_s reached a maximum of 0.84 ± 0.18 at 30.3 nm when TiO_2 concentration was 100 mg/L. The R_s then decreased from 0.84 ± 0.18 to 0.44 ± 1.2 as particle size increased from 30.3 to 45.8 nm. For both type and size, TiO_2 at concentration of 1000 mg/L had a greater effect on the R_s than at 100 mg/L, except for SiO_2 26 nm. The Al_2O_3 was at 1000 mg/L and the R_s was reduced from 0.44 ± 1.2 to 0.36 ± 0.05 as Al_2O_3 particle size was increased from 45.8 to 67.5 nm. The greatest impact on R_s by TiO_2 at 1000 mg/L was at d_1 of 46 nm with an R_s of 0.14 ± 0.09. Treatment with SiO_2 at 1000 mg/L concentration caused R_s to increase from 0.27 ± 0.01 to 1.1 ± 1.2 as particle size increased from 9.6 to 26 nm, respectively. The R_s decreased from 1.1 ± 0.12 at 26 nm to 0.64 ± 0.24 at 35.6 nm, in the presence of 1000 mg/L of SiO_2. The R_s responded similarly to 100 mg/L of Al_2O_3 and SiO_2. As both particles increased in d_1, the R_s increased. Figure 7 shows no apparent difference in the response between the two types of NP.

Figure 8 gives plots of the normalized specific chlorophyll a (Y) for Al_2O_3, SiO_2, and TiO_2 at several primary particle sizes and two particle concentrations (e.g., 100 and 1000 mg/L). Al_2O_3 at concentration of 100 mg/L increased the Y by an average of 71% between 15.8 and 17.6 nm. The largest Al_2O_3 at 100 mg/L increased the Y to 3.25 ± 2.16. Al_2O_3 at 15.8 nm and 1000 mg/L decreased the Y to 0.78 ± 0.70; however, this was not statistically different from the control. There was no difference between Al_2O_3 and the control with respect to concentration or size. SiO_2 at a concentration of 100 mg/L significantly increased the Y at all d_1 values compared to the control, except at 26 nm. SiO_2 at concentration of 1000 mg/L significantly decreased the Y by $84 \pm 4\%$ the control at all d_1 values. As d_1 value of TiO_2 at a concentration of 100 mg/L increased, the Y increased; however, the average Y at this treatment was not different from the control. The TiO_2 at 1000 mg/L increased the Y by a factor of 10 over the control level as the particle size increased from 4.8 to 30.3 nm.

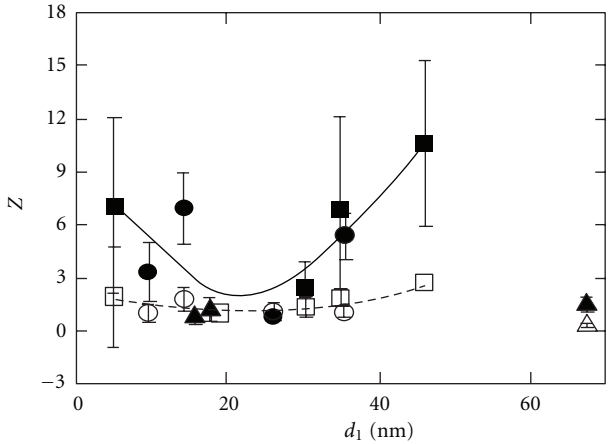


Figure 9: Normalized specific lipid oxidation (Z) for three types of NP. Circles are SiO_2, triangles are Al_2O_3, and squares are TiO_2. Open symbols are 100 mg/L. Solid symbols are 1000 mg/L. Line is fitted 4-parameter Gaussian equation (9) in SigmaPlot ver. 9.01. Experimental conditions: initial algae concentration = $1.4 \pm 0.9 \times 10^6$ cell/mL, test duration = 4 days, and initial test volume = 200 mL.

Figure 9 is a plot of normalized specific MDA (Z) at various d_1 values for Al_2O_3, SiO_2, and TiO_2 at two particle concentrations (e.g., 100 and 1000 mg/L). The Al_2O_3 at

a concentration of 100 mg/L resulted in an average Z of 1.39 ± 0.14. The maximum of 2.7 occurred for the TiO_2 concentration of 100 mg/L at 46 nm. The minimum of 0.29 occurred for the Al_2O_3 concentration of 1000 mg/L at 67.5 nm. The 1000 mg/L treatments significantly ($\alpha = 0.05$) increased normalized specific MDA for all samples, but SiO_2 at 26 nm. SiO_2 at 26 nm decreased the normalized specific MDA to 0.86 from control levels. Al_2O_3 at a concentration of 100 mg/L significantly ($\alpha = 0.05$) decreased the normalized specific MDA compared to the control. SiO_2 and TiO_2 at a concentration of 100 mg/L significantly ($\alpha = 0.001$) increased the normalized specific MDA compared to the control. The average normalized specific MDA for the 1000 mg/L of Al_2O_3 was 1.14 ± 0.13. This was significantly higher than the control ($\alpha = 0.05$). The SiO_2 and TiO_2 were fitted with (9), represented as lines in Figure 9:

$$Z = {d_1}^1 + a''' \exp\left[-0.5\left\{\frac{\left(d_1 - {d_1}^2\right)}{b''}\right\}^2\right], \quad (9)$$

where Z is the normalized specific lipid peroxidation, d_1 is the ENP size (nm), ${d_1}^2$ is the ENP size (nm) which the minimum value of Z occurs, a''' and b'' are fitting parameters, and y_0' is value at which the equation crosses the y intercept. Al_2O_3 was not included in model fitting because there were not differences in Z across the ENP size profile. This was as expected as Al_2O_3 is non-photocatalytic. The correlation coefficient (r^2) was 0.67 and 0.68 for 100 and 1000 mg/L, respectively. The average minimum value for the fitted equation occurs at 22.1 ± 0.3 nm for both 100 and 1000 mg/L treatments.

4. Discussion

The discussion will be divided into sections of different ENP materials. The sequence of the section will be from NP with the least number of influential factors (e.g., Al_2O_3) to that of the most number of influential factors (e.g., TiO_2). Factors such as water solubility, light availability, flocculation, photocatalytic properties, and ENP size that may impact the algae.

4.1. Aluminum Oxide. Aluminum oxide is the ENP with least number of influential factors in terms of the response by the algae and NP properties. The solubility of Al_2O_3 was not considered a factor in the toxicity seen in Figure 1. Unlike other NM such as CdSe that may bring about toxic metals such as Cd^{2+} [26, 27], Al_2O_3 would not generate enough Al^{3+} to cause the decreased growth. Gensemer and Playle [28] reported aluminum toxicity to *P. subcapitata* (formally known as *S. capricornutum*), with an EC value of 460 μg/L based on the biomass and 1,320 μg/L based on reduction of cell counts, respectively. The pH range of the above study was 7 to 8.2, which was similar to this study. Metal ions are considered the most bioavailable/toxic species [29]. Using equilibrium constant reported by Sparks [30], the concentration of (Al^{3+}) from solubility of γ–Al_2O_3(c) was calculated to be in the range between $10^{-12.5}$ mol/L at pH 8 and $10^{-9.5}$ mol/L at pH 7. The concentration was several orders of magnitude smaller than what caused significant responses in other algal studies and were not considered the cause of the adverse effects observed. Additionally, Al_2O_3 is not a photocatalyst. In Figures 3 and 9, the degree of lipid peroxidation was reduced compared to SiO_2 and TiO_2. The increase in Z (normalized specific MDA) for Al_2O_3 (Figure 3) is most likely due to measurements approaching the detection limits of the method ($\approx 0.2\,\mu$M as malondialdehyde-thiobarbituric acid complex (MDA-TBA)). In combination with low cell counts at high NP concentration, low MDA-TBA will give large variation in normalized specific lipd peroxidation, Z. This indicates that Al_2O_3 did not increase the ROS in the system. Therefore, ROS was also not considered a factor in Al_2O_3 toxicity.

Al_2O_3 NP did not affect the normalized specific lipid peroxidation, Z, or the chlorophyll a content of the *P. subcapitata* cells. However, Al_2O_3 NP did affect the growth of the algal cells. This disagreed with Ji et al. [6] who reported that nano-Al_2O_3 did not have a significant effect on *Chlorella* sp. Several factors that govern the effect of Al_2O_3 on algal growth included flocculation, light availability, nutrient availability, and primary particle size, d_1. First, flocculation was affected by the surface charge (i.e., pH_{pzc}) of both the algal cells and Al_2O_3 [31, 32]. Al_2O_3 has a pH_{pzc} of 8.2–9.1 [30] and *P. subcapitata* has a pH_{pzc} of about 2 [31]. The difference in pH_{pzc} between Al_2O_3 and algal cells will induce flocculation and increase the apparent density of the algae [31]. In turn, the ability of the algal cells to remain buoyant will decrease as seen with *Microcystis* spp. and clay aggregation [32]. In the absence of ENP, as algae cells settle in a pond or river, the light and nutrient availability will change [33]. In most cases, these changes do not favor algal growth [33]. Second, Al_2O_3 can influence the nutrient availability. Al_2O_3 can affect the nutrient availability due to adsorption [34]. Speohr and Milner [35] related the availability of nutrients to the chlorophyll content in algal cells (Figures 2 and 8). In this study the possible nutrient adsorption was most prevalent when Al_2O_3 concentration was greater than 100 mg/L (Figure 2). Finally, NP which has limited solubility under the experimental conditions will increase the turbidity of the test sample. This turbidity will cause a shading effect which will decrease the available light to the algae in photosynthesis [36]. Decreased available light has been shown to decrease chlorophyll content of algae in sponges and decrease growth rate of *D. tertiolecta*. The shading effect would be from the Al_2O_3 flocculated with the algae and those NP particles which remain unattached [31]. The flocculation between NP and the algae cells resulted in incomplete, multilayered surface coverage [31].

The effect of NP size on growth is seen in Figure 7. Increased growth occurred with increasing the primary particle size of Al_2O_3, d_1. Smaller particles will increase the turbidity of the suspension more than larger particles on the same mass basis, which will increase the effect of shading on the algal cells. The adsorption capacity of nutrients will be greater at smaller d_1 than larger d_1. With more nutrients being removed from the suspension, the algae will have reduced growth.

4.2. Silicon Dioxide. SiO_2 NM has the same influential factors (nutrient limiting, light limiting) as Al_2O_3 but has the additional effect on increasing the lipid peroxidation. Like Al_2O_3, the solubility of SiO_2 NP was not considered a factor affecting the EC value. Van Hoecke et al. [4] found that SiO_2 at particle size of 12.5 and 27.0 nm had a 72 h specific growth rate EC20 of 20.0 ± 5.0 and 28.8 ± 3.2 mg/L, respectively. Of the NP concentrations used in the Van Hoecke et al. [4] study, the highest concentration of dissolved Si was 4.1 mg/L at pH 7.5. The measured dissolved Si at EC20 in the present study was 234 mg/L, which was adequate to affect the growth of algae. Therefore, dissolved Si was not considered a major factor in SiO_2 toxicity. The difference in EC values between this work and that of Van Hoecke et al. [4] could be due to different initial algal densities. We used an initial cell density of 10^6 and Van Hoecke et al. [4] used 10^5 cell/mL. SiO_2 did not play a major role in the growth of *P. subcapitata* over the concentration range tested in ourwork, which agreed with Ji et al. [6] who reported little effect on *Chlorella* sp. Growth at SiO_2 concentration of 1000 mg/L in the size range of 20–50 nm.

SiO_2 caused an increase in lipid peroxidation (Figures 3 and 9). An increase in SiO_2 caused an increased average normalized specific lipid peroxidation, Z, (Figure 3). Although not considered a photocatalyst, SiO_2 has been observed to produce similar photosensitive effects, including increased ROS levels and reduced glutathione levels, as a photocatalyst [1]. In this study, the effect of SiO_2 NP on normalized specific MDA, Z, could be due more to limit light availability than the production of ROS directly. Limited light availability has been shown to produce $^1O_2$ under aerobic conditions through back flow of electrons to excite P_{680} to $^3P_{680}$ [37, 38]. Here P_{680} is the reaction center containing chlorophyll within the thylakoid membrane. The ROS generated in this reaction is responsible for increasing normalized specific lipid peroxidation, Z. The decrease in normalized specific MDA as the concentration of SiO_2 ENP increase was due to turbidity increase and light availability decrease as affected by the particle size. Rayleigh theory of light scattering predicts that light scattering is proportional to the ratio between the radius of a particle and a given wavelength of light with light scattering efficiency being proportional to the fourth power of particle radius [36]. This would reduce the back flow of electrons. The growth of cells at 1000 mg/L (Figure 7) was inversely proportional to the lipid peroxidation at 1000 mg/L (Figure 9). This was also affected by the lack of flocculation between the algae and the SiO_2 which resulted in evenly distributed shading effect throughout the algal cells.

SiO_2 affected the chlorophyll content of the algal cells (Figures 2 and 8). Low NP concentration increased Chla, whereas high NP concentration decreased it. Results showed that limited light availability can affect the chlorophyll content in algae [39, 40]. The reduction in light availability would encourage the algae to produce more chlorophyll per cell [41]. At low concentrations the algae will attempt to overcome the decreased light availability. Following the Rayleigh theory of light scattering, the turbidity of the solutions increased with decreased NP size on the same mass basis (Figure 8 open circles). With increased NP size the light availability to the algae increased; the less chlorophyll a the algae need to produce. The Chla was reduced significantly at 1000 mg/L SiO_2 (Figure 8). Manganese deficiency has been the cause of decreased chlorophyll content in *Chlorella fusca* and *Chlorella vulgaris* [42]. Nutrient limitation due to the adsorption of nutrients on SiO_2 may have caused the decreased Chla. The SiO_2 has a pH_{pzc} about 2, similar to that of algae. There have been many studies that show adsorption of cations to NM [43–45]. In particular, SiO_2 has shown to adsorb Mg(II), Mn(II), Na(I), K(I), Cu(II), and Zn(II) [30] which are all required nutrients from algal cell health.

4.3. Titanium Dioxide. TiO_2 is the NP with the most number of influential factors that affect the responses of *P. subcapitata*. TiO_2 with pH_{pzc} of 6.5 acted similarly to Al_2O_3 by flocculating with algae, adsorbing nutrients, and limiting light availability. TiO_2 also acted similarly to SiO_2 by having a portion of the NP remain free in suspension, limiting light availability and affecting lipid peroxidation. However, unlike SiO_2, TiO_2 is a known photocatalyst that generates ROS.

NP is soluble in water leading to release of metal ions (M^{n+}) ions, which are toxic to organisms [28, 29]. This could not be a key factor in the case of TiO_2. There is little information regarding the toxicity of Ti^{4+}. Thermodynamically, the formation of Ti^{4+} in aqueous solution will be limited due to the formation of dissolved TiO_2 [46]. This will have minimal effect on organisms because of the small percent of total metal that is present as free metal ion. Therefore, the solubility of TiO_2 was not a major factor controlling the responses of algae to this NP.

Major factors affecting the algal responses include light availability, flocculation, particle size, and photoactivity. These factors are interrelated. When TiO_2 and algal cells are introduced into the suspension, flocculation takes place right away [31]. Like Al_2O_3, TiO_2 will affect the apparent density of the algal cells. Flocculation between algal cells and TiO_2 was observed and was consistent with Lin [31] which reported absorption of TiO_2 to *P. subcapitata*. The flocculation with TiO_2 has the effect of bringing the algae in direct contact with the ROS-generating TiO_2 (Figure 3). The lipid peroxidation may have been affected by the adsorption of NP to the surface of the algal cells. The direct transfer of ROS from the point of generation to the surface of algal cells is important. This can be exemplified by calculating the distance highly reactive hydroxyl radical ($OH^\bullet$) will travel before it reaches the end of the first half-life. The half-life of ROS is on the order of milliseconds [47, 48]. Lee et al. [49] used the diffusion layer thickness of 800 nm to calculate Ag^+ diffusion to *P. subcapitata*. The hydroxyl radical ($OH^\bullet$) diffusion coefficient is 2.3×10^{-9} m^2/s [50]. From Fick's second law of diffusion and assuming the reaction rate of $OH^\bullet$ is on the order of milliseconds, then the $OH^\bullet$ would travel approximately 18 nm before one half of the $OH^\bullet$ would react with other oxygen species in the water. The concentration of $OH^\bullet$ would be reduced by >99% by the time and would diffuse to the surface of the algal cell. It is feasible that if the NP and algae are not in contact, the ROS will not bring about lipid peroxidation. The lipid peroxidation was maximized at d_1 of 42 nm (Figure 6) which correlates with the maximum size

effect on growth (Figure 4). The number of particles that flocculate with an algal cell might be correlated to d_1. Larger d_1 might decrease the number of NP that will flocculate with algae. This will also affect available light. The incomplete, multilayered coverage of the algal cells, like Al_2O_3, may decrease light availability to the algal cells. As discussed with Al_2O_3 and SiO_2, the decrease in light will affect the growth and chlorophyll content.

The primary particle size of TiO_2, d_1, played a role in algal growth, chlorophyll content of algal cells, and lipid peroxidation of algal cells (Figures 4–6). All of these endpoints have maximum effect values at the same particle size of 42 nm. Like Al_2O_3 and SiO_2, nutrients such as Cu, Fe, or N would be imitated due to the scavenged by NP, which in turn could affect the chlorophyll content. It has been suggested that NP can decrease bioavailability of nutrients, which would contribute to toxicity [6]. The smaller the d_1, the greater the specific surface area and the more nutrients would be adsorbed. Gao et al. [51] observed that maximum adsorption density of Cd^{2+} (Γ_{max}) varied inversely proportional to the NP size. That relationship would be true for nutrients such as Cu, Fe, or N, which in turn would affect the chlorophyll a production and algal growth [35]. The d_1 primarily affect the critical specific chlorophyl (Figure 5). Lin [31] studied the adsorption of TiO_2 onto *P. subcapitata* and reported that at pH 7.3 and initial TiO_2 of 150 mg/L, the TiO_2 uptake (no. TiO_2 per algal cell) was constant at 3×10^5 TiO_2 particles per algal cell. At higher concentration of TiO_2, there will be no additional uptake.

The extent of lipid peroxidation has been related to the amount of reactive oxygen species in many different systems including humans to fish to bacteria [43–55]. Generation of ROS by NP photocatalysts is related to the size and the type of NP [10, 56]. Size of the particles controls the band gap and surface area [8, 11]. The band gap determines the level of light energy that is converted to protons and the surface area affects the recombination of election-hole pairs. Many studies have shown that optimum degradation of organic compounds occurs of TiO_2 between 3.8 and 40 nm [36, 57–61]. These values are smaller than what is observed in Figure 6. The lipid peroxidation in this study may be influenced by adsorption of NP to the surface of the algae. The half-life of ROS is on the order of microseconds, for example, the superoxide anion ($^{\bullet}O_2^-$) has a half-life of 1 μs and hydrogen peroxide (H_2O_2) has a half-life of 1 ms [48, 49]. Due to this time scale, it is feasible that if the NP and algae are not in contact, the ROS will not prompt lipid peroxidation. However, no literature was available regarding how d_1 affects the aggregation between algae and NP. Additionally, light availability is being optimized for ROS generation at d_1 of ca. 42 nm. At d_1 smaller than 42 nm, the surface density of particles increases, which decreases the light availability to the NP in direct contact with the surface of the cells.

5. Conclusions

This research was undertaken to answer the following questions. How toxic is the TiO_2 to algae? What does NP size play in toxicity? Does the type of NP play a role in toxicity, chlorophyll content, and lipid peroxidation?

The effects of photocatalytic TiO_2 on algae was compared to that of non-photocatalytic nanoparticles (e.g., Al_2O_3 and SiO_2). Based on results, it can be concluded that TiO_2 is "harmful-toxic" between a d_1 of 30 to 60 nm and nontoxic at $d_1 < 30$ nm and $d_1 > 60$ nm. The term harmful is defined as measurement endpoints from 10–100 mg/L [62]. The term non-toxic is defined as measurement endpoints >100 mg/L [62]. The most important factor was the surface charge of the material as it affected the aggregation between algae and NP, which in turn affected lipid peroxidation, chlorophyll a content, and growth.

If nanoparticles were released into the environment, algae would be flocculated dependent on the extent of surface charge of the nanoparticles and the algal cells. The algae will attempt to overcome the shading effect by increasing the chlorophyll content in order to optimize the light availability. With a high degree of light scattering, that is, limited light availability, lipid peroxidation may be generated by "back flow of electrons in the PSII from the semiquinone acceptor to the $S_{2,3}$ oxidation states of the donor side" [37]. Additionally, as the algae are removed from the water column by an increased rate of settling, the light availability will continue to decrease. Exposure time in the water column will be limited, in most cases, due to flocculation and subsequent settling out of nanoparticles in the water column.

Lipid peroxidation was the only measurement used to determine reactive oxygen species activity. However, it is suggested that several additional biochemical markers be measured in order to observe how the defensive mechanism response of algae in response to nanoparticles. It is therefore suggested that subchronic endpoints be a measurement for future work, including, but not limited to, glutathione, superoxide dismutase, and various direct ROS assays. Additionally, the response of several additional species of algae is recommended for the purpose of comparison. This will add in verifying the results of this study.

Acknowledgments

Dr. Y. L. Liao, a visiting scholar from Taiwan, synthesized TiO_2 nanoparticles of various sizes used in this study. This paper was funded by USEPA STAR Grant no. R-83172101. Dr. Nora Savage was the project manager. Results, discussions, and conclusions are those of the authors and should not be interpret, as endorsement of the funding agency. Sources of nanoparticles studied came from the following suppliers: Degussa Corp., Allied High Tech Products, Nanostructured and Amorphous Materials, Inc., and Sachtleben Chemicals. The authors have no direct financial interest in or relationship with any of the above companies.

References

[1] W. Lin, Y. W. Huang, X. D. Zhou, and Y. Ma, "In vitro toxicity of silica nanoparticles in human lung cancer cells," *Toxicology and Applied Pharmacology*, vol. 217, pp. 252–259, 2006.

[2] A. J. Wagner, C. A. Bleckmann, R. C. Murdock, A. M. Schrand, J. J. Schlager, and S. M. Hussain, "Cellular interaction of different forms of aluminum nanoparticles in rat alveolar macrophages," *Journal of Physical Chemistry B*, vol. 111, no. 25, pp. 7353–7359, 2007.

[3] M. Bodo, G. Muzi, C. Bellucci et al., "Comparative in vitro studies on the fibrogenic effects of two samples of silica on epithelial bronchial cells," *Journal of Biological Regulators and Homeostatic Agents*, vol. 21, no. 3-4, pp. 97–104, 2007.

[4] K. Van Hoecke, K. A. C. De Schamphelaere, P. Van der Meeren, S. Lucas, and C. R. Janssen, "Ecotoxicity of silica nanoparticles to the green alga *Pseudokirchneriella subcapitata*: importance of surface area," *Environmental Toxicology and Chemistry*, vol. 27, no. 9, pp. 1948–1957, 2008.

[5] D. B. Warheit, T. R. Webb, K. L. Reed, S. Frerichs, and C. M. Sayes, "Pulmonary toxicity study in rats with three forms of ultrafine-TiO_2 particles: differential responses related to surface properties," *Toxicology*, vol. 230, no. 1, pp. 90–104, 2007.

[6] J. Ji, Z. Long, and D. Lin, "Toxicity of oxide nanoparticles to the green algae *Chlorella sp*.," *Chemical Engineering Journal*, vol. 170, pp. 525–530, 2011.

[7] E. Pinto, T. C. S. Sigaud-Kutner, M. A. S. Leitão, O. K. Okamoto, D. Morse, and P. Colepicolo, "Heavy metal-induced oxidative stress in algae," *Journal of Phycology*, vol. 39, no. 6, pp. 1008–1018, 2003.

[8] L. Brus, "Electronic wave functions in semiconductor clusters: experiment and theory," *Journal of Physical Chemistry*, vol. 90, no. 12, pp. 2555–2560, 1986.

[9] Y. H. Tseng, H. Y. Lin, C. S. Kuo, Y. Y. Li, and C. P. Huang, "Thermostability of Nano-TiO_2 and its photocatalytic activity," *Reaction Kinetics and Catalysis Letters*, vol. 89, pp. 63–69, 2006.

[10] S. Bakardjieva, J. Šubrt, V. Štengl, M. J. Dianez, and M. J. Sayagues, "Photoactivity of anatase-rutile TiO_2 nanocrystalline mixtures obtained by heat treatment of homogeneously precipitated anatase," *Applied Catalysis B*, vol. 58, no. 3-4, pp. 193–202, 2005.

[11] H. Lin, C. P. Huang, W. Li, C. Ni, S. I. Shah, and Y. H. Tseng, "Size dependency of nanocrystalline TiO_2 on its optical property and photocatalytic reactivity exemplified by 2-chlorophenol," *Applied Catalysis B*, vol. 68, pp. 1–11, 2006.

[12] C. Y. Liu and A. J. Bard, "Effect of excess charge on band energetics (optical absorption edge and carrier redox potentials) in small semiconductor particles," *Journal of Physical Chemistry*, vol. 93, no. 8, pp. 3232–3237, 1989.

[13] J. M. Nedeljković, M. T. Nenadović, O. I. Mićić, and A. J. Nozik, "Enhanced photoredox chemistry in quantized semiconductor colloids," *Journal of Physical Chemistry*, vol. 90, no. 1, pp. 12–13, 1986.

[14] U. Koch, A. Fojtik, H. Weller, and A. Henglein, "Photochemistry of semiconductor colloids. Preparation of extremely small ZnO particles, fluorescence phenomena and size quantization effects," *Chemical Physics Letters*, vol. 122, no. 5, pp. 507–510, 1985.

[15] F. Morazzoni, C. Canevali, N. Chiodini et al., "Nanostructured Pt-doped tin oxide films: sol-gel preparation, spectroscopic and electrical characterization," *Chemistry of Materials*, vol. 13, no. 11, pp. 4355–4361, 2001.

[16] R. Hardman, "A toxicologic review of quantum dots: toxicity depends on physicochemical and environmental factors," *Environmental Health Perspectives*, vol. 114, no. 2, pp. 165–172, 2006.

[17] S. Kashiwada, "Distribution of nanoparticles in the see-through medaka (Oryzias latipes)," *Environmental Health Perspectives*, vol. 114, no. 11, pp. 1697–1702, 2006.

[18] L. K. Adams, D. Y. Lyon, and P. J. J. Alvarez, "Comparative ecotoxicity of nanoscale TiO_2, SiO_2, and ZnO water suspensions," *Water Research*, vol. 40, no. 19, pp. 3527–3532, 2006.

[19] United States Environmental Protection Agency, "Short-term methods for estimating the chronic toxicity of effluents and receiving waters to freshwater organisms," Tech. Rep. EPA-821-R-02-013, United States Environmental Protection Agency, Office of Water, Washington, DC, USA, 2002.

[20] D. Metzler, *Effect of Food-Borne Cadmium on the Reproduction of Ceriodaphina Dubia [M.S. thesis]*, University of Delaware, Newark, Del, USA, 2003.

[21] C. I. Weber, L. A. Fay, G. B. Collins, D. E. Rathke, and J. Tobin, "A review of methods for the analysis of chlorophyll in periphyton and plankton of marine and freshwater systems," Tech. Rep. Technical bulletin OHSU-TB-15, Ohio State University Sea Grant Program, 1986.

[22] A. D. Eaton, L. S. Clesceri, and A. E. Greenberg, *Standard Methods for the Examination of Water and Wastewater*, American Public Health Association, American Water Works Association, and Water Environment Federation, Washington, DC, USA, 19th edition, 1995.

[23] P. C. Maness, S. Smolinski, D. M. Blake, Z. Huang, E. J. Wolfrum, and W. A. Jacoby, "Bactericidal activity of photocatalytic TiO_2 reaction: toward an understanding of its killing mechanism," *Applied and Environmental Microbiology*, vol. 65, no. 9, pp. 4094–4098, 1999.

[24] United States Environmental Protection Agency, *Toxicity Relationship Analysis Program. Version 1*, United States Environmental Protection Agency, National Health and Environmental Effects Research Laboratory, Mid-continent Ecology Division, Duluth, Minn, USA, 2002.

[25] A. M. M. Goncalves, D. R. de Figureueiredo, and M. J. Pereira, "The effects of different salinity concentrations on growth of three freshwater green algae," *Fresenius Environmental Bulletin*, vol. 15, no. 11, pp. 1382–1386, 2006.

[26] S. H. Hsieh, K. P. Tsai, and C. Y. Chen, "The combined toxic effects of nonpolar narcotic chemicals to *Pseudokirchneriella subcapitata*," *Water Research*, vol. 40, no. 10, pp. 1957–1964, 2006.

[27] C. Kirchner, T. Liedl, S. Kudera et al., "Cytotoxicity of colloidal CdSe and CdSe/ZnS nanoparticles," *Nano Letters*, vol. 5, no. 2, pp. 331–338, 2005.

[28] R. W. Gensemer and R. C. Playle, "The bioavailability and toxicity of aluminum in aquatic environments," *Critical Reviews in Environmental Science and Technology*, vol. 29, no. 4, pp. 315–450, 1999.

[29] H. E. Allen, R. H. Hall, and T. D. Brisbin, "Metal speciation. Effects on aquatic toxicity," *Environmental Science and Technology*, vol. 14, no. 4, pp. 441–443, 1980.

[30] D. Sparks, *Environmental Soil Chemistry*, Academic Press, New York, NY, USA, 2nd edition, 2003.

[31] M. Y. Lin, *Interactions between Titanium Dioxide Nanoparticles and Algal Cells at Moderate Particle Concentration [M.S. thesis]*, University of Delaware, Newark, Del, USA, 2008.

[32] J. M. H. Verspagen, J. Passarge, K. D. Jöhnk et al., "Water management strategies against toxic *Microcystis* blooms in the Dutch delta," *Ecological Applications*, vol. 16, no. 1, pp. 313–327, 2006.

[33] R. G. Wetzel and, *Limnology*, Saunders College, New York, NY, USA, 2nd edition, 1985.

[34] S.-F. Cheah, G. E. Brown Jr., and G. A. Parks, "XAFS spectroscopy study of Cu(II) sorption on amorphous SiO_2 and gamma-Al_2O_3: effect of substrate and time on sorption complexes," *Journal of Colloid and Interface Science*, vol. 208, no. 1, pp. 110–128, 1998.

[35] H. A. Speoher and H. W. Milner, "The chemical composition of Chlorella; effect of environmental conditions," *Plant Physiology*, vol. 24, no. 1, pp. 120–149, 1949.

[36] A. J. Maira, K. L. Yeung, C. Y. Lee, P. L. Yue, and C. K. Chan, "Size effects in gas-phase photo-oxidation of trichloroethylene using nanometer-sized TiO_2 catalysts," *Journal of Catalysis*, vol. 192, no. 1, pp. 185–196, 2000.

[37] N. Keren, A. Berg, P. J. M. Van Kan, H. Levanon, and I. Ohad, "Mechanism of photosystem II photoinactivation and D1 protein degradation at low light: the role of back electron flow," *Proceedings of the National Academy of Sciences of the United States of America*, vol. 94, no. 4, pp. 1579–1584, 1997.

[38] Y. Nishiyama, S. I. Allakhverdiev, and N. Murata, "Inhibition of the repair of Photosystem II by oxidative stress in cyanobacteria," *Photosynthesis Research*, vol. 84, no. 1–3, pp. 1–7, 2005.

[39] T. E. Brown and F. L. Richardson, "The effect of growth environment on the physiology of algae: light intensity," *Journal of Phycology*, vol. 4, pp. 38–54, 1968.

[40] M. J. Behrenfeld, O. Prasil, M. Babin, and F. Bruyant, "In search of a physiological basis for covariations in light-limited and light-saturated photosynthesis," *Journal of Phycology*, vol. 40, no. 1, pp. 4–25, 2004.

[41] M. F. Colombo-Pallotta, E. García-Mendoza, and L. B. Ladah, "Photosynthetic performance, light absorption, and pigment composition of *Macrocystis pyrifera* (Laminariales, Phaeophyceae) blades from different depths," *Journal of Phycology*, vol. 42, no. 6, pp. 1225–1234, 2006.

[42] E. Kessler, "Effect of manganese deficiency on growth and chlorophyll content of algae with and without hydrogenase," *Archiv für Mikrobiologie*, vol. 63, no. 1, pp. 7–10, 1968.

[43] K. Hristovski, A. Baumgardner, and P. Westerhoff, "Selecting metal oxide nanomaterials for arsenic removal in fixed bed columns: from nanopowders to aggregated nanoparticle media," *Journal of Hazardous Materials*, vol. 147, no. 1-2, pp. 265–274, 2007.

[44] P. Liang, Y. Qin, B. Hu, C. Li, T. Y. Peng, and Z. Jiang, "Study of the adsorption behavior of heavy metal ions on nanometer-size titanium dioxide with ICP-AES," *Fresenius' Journal of Analytical Chemistry*, vol. 368, no. 6, pp. 638–640, 2000.

[45] E. Vassileva, K. Hadjiivanov, T. Stoychev, and C. Daiev, "Chromium speciation analysis by solid-phase extraction on a high surface area TiO_2 ," *Analyst*, vol. 125, no. 4, pp. 693–698, 2000.

[46] W. Stumm and J. J. Morgan, *Aquatic Chemistry: Chemical Equilibria and Rates in Natural Waters*, John Wiley and Sons, New York, NY, USA, 3rd edition, 1996.

[47] M. Reth, "Hydrogen peroxide as second messenger in lymphocyte activation," *Nature Immunology*, vol. 3, no. 12, pp. 1129–1134, 2002.

[48] M. Drábková, B. Maršálek, and W. Admiraal, "Photodynamic therapy against cyanobacteria," *Environmental Toxicology*, vol. 22, no. 1, pp. 112–115, 2007.

[49] D. Y. Lee, C. Fortin, and P. G. Campbell, "Influence of chloride on silver uptake by two green algae, Pseudokirchneriella subcapitata and *Chlorella pyrenoidosa*," *Environmental Toxicology and Chemistry*, vol. 23, no. 4, pp. 1012–1018, 2004.

[50] I. M. Svishchev and A. Y. Plugatyr, "Hydroxyl radical in aqueous solution: computer simulation," *Journal of Physical Chemistry B*, vol. 109, no. 9, pp. 4123–4128, 2005.

[51] Y. Gao, R. Wahi, A. T. Kan, J. C. Falkner, V. L. Colvin, and M. B. Tomson, "Adsorption of cadmium on anatase nanoparticles-effect of crystal size and pH," *Langmuir*, vol. 20, no. 22, pp. 9585–9593, 2004.

[52] F. Wolfe-Simon, D. Grzebyk, O. Schofield, and P. G. Falkowski, "The role and evolution of superoxide dismutases in algae," *Journal of Phycology*, vol. 41, no. 3, pp. 453–465, 2005.

[53] C. M. Sayes, A. M. Gobin, K. D. Ausman, J. Mendez, J. L. West, and V. L. Colvin, "Nano-C_{60} cytotoxicity is due to lipid peroxidation," *Biomaterials*, vol. 26, no. 36, pp. 7587–7595, 2005.

[54] A. Valavanidis, T. Vlahogianni, M. Dassenakis, and M. Scoullos, "Molecular biomarkers of oxidative stress in aquatic organisms in relation to toxic environmental pollutants," *Ecotoxicology and Environmental Safety*, vol. 64, no. 2, pp. 178–189, 2006.

[55] K. Kato, A. Tsuzuki, H. Taoda, Y. Torii, T. Kato, and Y. Butsugan, "Crystal structures of TiO_2 thin coatings prepared from the alkoxide solution via the dip-coating technique affecting the photocatalytic decomposition of aqueous acetic acid," *Journal of Materials Science*, vol. 29, no. 22, pp. 5911–5915, 1994.

[56] M. Anpo, H. Nakaya, S. Kodama, Y. Kubokawa, K. Domen, and T. Onishi, "Photocatalytic hydrogenation of propyne with water on small-particle titania: size quantization effects and reaction intermediates," *The Journal of Physical Chemistry*, vol. 91, no. 16, pp. 4305–4310, 1987.

[57] K. Tanaka, M. F. V. Capule, and T. Hisanaga, "Effect of crystallinity of TiO_2 on its photocatalytic action," *Chemical Physics Letters*, vol. 187, no. 1-2, pp. 73–76, 1991.

[58] Z. Zhang, C. C. Wang, R. Zakaria, and J. Y. Ying, "Role of particle size in nanocrystalline TiO_2-based photocatalysts," *Journal of Physical Chemistry B*, vol. 102, no. 52, pp. 10871–10878, 1998.

[59] J. K. Yang and A. P. Davis, "Competitive photocatalytic oxidation of Cu(II)—EDTA and Cd(II)—EDTA with illuminated TiO_2 ," *Environmental Science and Technology*, vol. 35, no. 17, pp. 3566–3570, 2001.

[60] C. B. Almquist and P. Biswas, "Role of synthesis method and particle size of nanostructured TiO_2 on its photoactivity," *Journal of Catalysis*, vol. 212, no. 2, pp. 145–156, 2002.

[61] H. J. Nam, T. Amemiya, M. Murabayashi, and K. Itoh, "Photocatalytic activity of sol-gel TiO_2 thin films on various kinds of glass substrates: the effects of Na^+ and primary particle size," *Journal of Physical Chemistry B*, vol. 108, no. 24, pp. 8254–8259, 2004.

[62] C. Blaise, F. Gagné, J. F. Férard, and P. Eullaffroy, "Ecotoxicity of selected nano-materials to aquatic organisms," *Environmental Toxicology*, vol. 23, no. 5, pp. 591–598, 2008.

[63] C. D. Dong, Y. L. Liao, C. M. Kao, C. W. Chen, H. Y. Lin, and C. P. Huang, "Preparation of crystalline nanosized titania by microemulsion: evaluation of process variables," *Advanced Oxidation Technology*, vol. 10, no. 2, pp. 399–404, 2007.

[64] Aerosil, September 2009, http://www.aerosil.com/wps/PA_1_2_1RD/downloadMsds?id=6.

[65] A. K. Arora and Kamaluddin, "Role of metal oxides in chemical evolution: interaction of ribose nucleotides with alumina," *Astrobiology*, vol. 9, no. 2, pp. 165–171, 2009.

[66] K. Bourikas, T. Hiemstra, and W. H. Van Riemsdijk, "Ion pair formation and primary charging behavior of titanium oxide (anatase and rutile)," *Langmuir*, vol. 17, no. 3, pp. 749–756, 2001.